Article:

Lan, X., Liu, W. and Ngan, H. (2020) Joint DOA and polarisation estimation with crossed-dipole and tripole sensor arrays. IEEE Transactions on Aerospace and Electronic Systems, 56 (6). pp. 4965-4973. ISSN: 0018-9251

https://doi.org/10.1109/TAES.2020.2990571

Joint DOA and Polarisation Estimation with Crossed-dipole and Tripole Sensor Arrays

Xiang Lan, Wei Liu, *Senior Member, IEEE,* and Henry Y. T. Ngan, *Senior Member, IEEE*

***Abstract*—Electromagnetic vector sensor arrays can track both the polarisation and direction of arrival (DOA) of the impinging signals. For linear crossed-dipole arrays, as shown by our analysis, due to inherent limitation of the structure, it can only track one DOA parameter and two polarisation parameters. For full four-dimensional (4-D, 2 DOA and 2 polarization parameters) estimation, we could extend the linear crossed-dipole array to the planar case. In this paper, instead of extending the array geometry, we replace the crossed-dipoles by tripoles and construct a linear tripole array. Detailed proof shows that such a structure can estimate the 2-D DOA and 2-D polarisation information effectively in general. A brief comparison between the planar crossed-dipole array and the linear tripole array is performed at last, showing that although the planar structure has a better performance, it is achieved at the cost of increased physical size.**

Keywords—linear tripole array, linear crossed-dipole array, direction of arrival (DOA), polarisation estimation.

I. Introduction

The joint estimation of direction of arrival (DOA) and polarisation for signals based on electromagnetic (EM) vector sensor arrays has been widely studied in the past [1]–[21]. In [1], the EM vector sensor was first used to collect both electric and magnetic information of the impinging signals, where all six electromagnetic components are measured to identify the signals. So far most of the studies are focused on the linear structure employing crossed-dipoles [2]–[4] and tripole sensors [5]–[8], where the general two-dimensional (2-D) DOA model is simplified into one-dimensional (1-D) by assuming that all the signals arrive from the same known azimuth angle ϕ. In [22], [23], MUSIC algorithm was proposed to deal with the joint DOA (θ) and polarisation (ρ, ϕ) estimation problem by considering DOA (1-D) and polarisation (2-D) together, where a three (3-D) peak search is required with a very high computational complexity. In [9], [10], [24]–[26], methods were developed so that the DOA and polarisation can be estimated separately.

In practice, the azimuth angle θ and the elevation angle ϕ of the signals are unknown and they are usually different for different signals and need to be estimated together. The existing 3-D joint DOA and polarisation work could be extended to four-dimensional (4-D) (2 DOA and 2 polarisation parameters). However, the 4-D estimation work comes with a uniqueness problem [27]–[32]. In [27], it indicates that the problem is due to the linear dependence of joint steering vectors. In [32] and [29], Tan proved that for an EM vector sensor and EM vector sensor array, every three joint steering vectors with different DOAs are linearly independent, while the fourth one with a different DOA could be the linear combination of the first three steering vectors. The linear dependence of steering vectors with tripole sensors is discussed in [30], where a special case of linear dependence is introduced that with some strict constraints, two steering vectors with different DOAs may be in parallel with each other, which can be avoided if the signals are nonlinearly polarised and arrives strictly from a hemispherical space.

When further reducing the tripole sensor array to a cross-dipole sensor array, as rigorously proved for the first time in this work, the linear crossed-dipole array has the parallel ambiguity problem, where the azimuth angle and the elevation angle of the impinging signals can not be uniquely identified. To tackle this problem, one solution is to extend the linear geometry to a 2-D array, such as the uniform rectangular array (URA) [33]. On the other hand, it is possible to add one dipole to the crossed-dipole structure to form a tripole sensor, and tripole sensor arrays have been proposed in the past for DOA estimation [34], [35]. Therefore, as another solution, motivated by simultaneously simplifying the array structure and reducing the computational complexity, the crossed-dipoles were replaced by tripoles and a linear tripole array was constructed in our earlier conference publication for joint 4-D DOA and polarisation estimation for the first time [36]. Moreover, for the first time, we give a clear proof about why a linear tripole array can be used for 4-D joint DOA and polarisation estimation, while avoiding the ambiguity problem except for some special cases.

As a URA of cross-dipoles can also achieve effective 4-D estimation, it would be interesting to know that given the same number of dipoles, which structure performs better. Our simulation results show that the URA has a better performance, at the cost of increased physical size. This observation is also verified by their Cramér-Rao Bounds [38]–[47].

This paper is structured as follows. The linear tripole array is introduced in Section II with a detailed proof for the 4-D ambiguity problem of non-linearly polarised signals associated with the linear crossed-dipole array and why the linear tripole array can solve the problem; for linearly polarised signals, the ambiguity exists even with tripole arrays and the case is analysed in detail. Simulation results are presented in Section III, and conclusions are drawn in Section IV.

X. Lan and W. Liu are with the Department of Electronic and Electrical Engineering, University of Sheffield, Sheffield, S1 3JD, UK (e-mail: {xlan2, w.liu}@sheffield.ac.uk). W. Liu is the corresponding author.

H. Ngan was with the Department of Mathematics. Hong Kong Baptist University, Hong Kong (e-mail: ngan.henry@gmail.com).

II. Tripole Sensor Array Model

A. Tripole sensor array

Suppose there are M uncorrelated narrowband signals impinging upon a uniform linear array with N tripoles, as shown in Fig. 1. Assume that all signals are stationary and nonlinearly-polarised (elliptically or circularly polarised). The parameters, including DOA and polarisation of the m-th signal are denoted by $(\theta_m, \phi_m, \gamma_m, \eta_m), m = 1, 2, ..., M$, where $\theta_m \in [0, \pi/2]$, $\phi_m \in [0, 2\pi]$. The inter-element spacing d is usually $\lambda/2$, where λ is the signal wavelength. For each tripole sensor, the three components are parallel to x, y and z axes, respectively. The background noise is white Gaussian with zero mean and variance σ_n^2, uncorrelated with the impinging signals. The steering vector for the m-th signal can be denoted as

$$\boldsymbol{a}_m = [1, e^{-j\pi \sin\theta_m \sin\phi_m}, ..., e^{-j(N-1)\pi \sin\theta_m \sin\phi_m}] \quad (1)$$

and the polarisation vector $\boldsymbol{p}_m$ is determined by the product of DOA component $\boldsymbol{\Omega}_m$ and the polarization component $\boldsymbol{g}_m$ [48], i.e.,

$$\boldsymbol{p}_m = \boldsymbol{\Omega}_m \boldsymbol{g}_m \quad (2)$$

with

$$\boldsymbol{\Omega}_m = \begin{bmatrix} \cos\theta_m \cos\phi_m & -\sin\phi_m \\ \cos\theta_m \sin\phi_m & \cos\phi_m \\ -\sin\theta_m & 0 \end{bmatrix} \quad (3)$$

$$\boldsymbol{g}_m = \begin{bmatrix} \sin\gamma_m e^{j\eta_m} \\ \cos\gamma_m \end{bmatrix} \quad (4)$$

where γ_m is the auxiliary polarization angle and η_m the polarization phase difference. By expanding (2), $\boldsymbol{p}_m$ can be divided into three different components in x, y and z axes

$$\boldsymbol{p}_m = \begin{bmatrix} \cos\theta_m \cos\phi_m \sin\gamma_m e^{j\eta_m} - \sin\phi_m \cos\gamma_m \\ \cos\theta_m \sin\phi_m \sin\gamma_m e^{j\eta_m} + \cos\phi_m \cos\gamma_m \\ -\sin\theta_m \sin\gamma_m e^{j\eta_m} \end{bmatrix} \quad (5)$$

For convenience, we replace the three elements in $\boldsymbol{p}_m$ by

$$\begin{aligned} p_{mx} &= \cos\theta_m \cos\phi_m \sin\gamma_m e^{j\eta_m} - \sin\phi_m \cos\gamma_m \\ p_{my} &= \cos\theta_m \sin\phi_m \sin\gamma_m e^{j\eta_m} + \cos\phi_m \cos\gamma_m \\ p_{mz} &= -\sin\theta_m \sin\gamma_m e^{j\eta_m} \end{aligned} \quad (6)$$

The received signal can be denoted as a function of steering vector $\boldsymbol{a}_m$, polarisation vector $\boldsymbol{p}_m$, source signals $s_m(t)$ and background noise $\boldsymbol{n}$. At the k-th time instant, the received signal vector $\boldsymbol{x}[k]$ can be expressed as

$$\begin{aligned} \boldsymbol{x}[k] &= \sum_{m=1}^{M} [\boldsymbol{a}_m \otimes \boldsymbol{p}_m] s_m[k] + \boldsymbol{n}[k] \\ &= \sum_{m=1}^{M} \boldsymbol{v}_m s_m[k] + \boldsymbol{n}[k] \end{aligned} \quad (7)$$

where $\otimes$ stands for the Kronecker product, $\boldsymbol{v}_m$ is the Kronecker product of $\boldsymbol{a}_m$ and $\boldsymbol{p}_m$, and $\boldsymbol{n}[k]$ is the $3N \times 1$ Gaussian white noise vector. The covariance matrix $\boldsymbol{R}$ is given by

$$\begin{aligned} \boldsymbol{R} &= E\{\boldsymbol{x}[k]\boldsymbol{x}[k]^H\} \\ &= \sum_{m=1}^{M} \boldsymbol{v}_m E\{s[k]s[k]^*\} \boldsymbol{v}_m^H + \sigma_n^2 \boldsymbol{I}_{3N} \end{aligned} \quad (8)$$

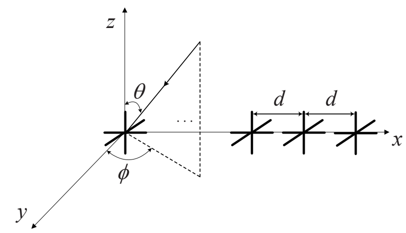

Fig. 1. Geometry of a uniform linear tripole array.

In practice, an estimated covariance matrix $\hat{\boldsymbol{R}}$ is used

$$\hat{\boldsymbol{R}} \approx \frac{1}{K} \sum_{l=1}^{L} \boldsymbol{x}[k]\boldsymbol{x}[k]^H \quad (9)$$

where K is the number of snapshots.

B. Comparison between Crossed-dipole and Tripole Arrays

This section will mainly show why the ULA with crossed-dipoles cannot uniquely determine the four parameters associated with each impinging signal, leading to the spatial aliasing problem, and why the ULA with tripoles can provide a unique solution for the joint 4-D estimation problem.

To show the ambiguity problem, consider one source signal impinging upon the array so that the subscript m can be dropped for convenience. The joint DOA and polarisation estimation problem can be considered as an estimation of the steering vector of this source signal.

For crossed-dipole sensor array, its joint steering vector $\boldsymbol{w}$ is given by

$$\boldsymbol{w} = \boldsymbol{a} \otimes \boldsymbol{q} \quad (10)$$

where

$$\boldsymbol{q} = [p_x, p_y]^T. \quad (11)$$

Here, $\boldsymbol{w}$ is a $2N \times 1$ vector with a 2×1 polarisation vector $\boldsymbol{q}$. For the tripole sensor array, the joint steering vector $\boldsymbol{v}$ is a $3N \times 1$ vector with a 3×1 polarisation vector $\boldsymbol{p}$, i.e.

$$\boldsymbol{v} = \boldsymbol{a} \otimes \boldsymbol{p} \quad (12)$$

where

$$\boldsymbol{p} = [p_x, p_y, p_z]^T. \quad (13)$$

For convenience, we use $\alpha = (\theta, \phi, \gamma, \eta)$ to denote the four parameters. The ambiguity problem associated with the cross-dipole array can be stated as follows: If there is an arbitrarily polarised signal from α_1, we can always find another signal from α_2 that satisfies $\boldsymbol{w}_1 // \boldsymbol{w}_2$, with $\alpha_1 \neq \alpha_2$, where // means the two vectors are in parallel, i.e., $\boldsymbol{w}_2 = k \cdot \boldsymbol{w}_1$, with k being an arbitrary complex-valued scalar.

When we say that the tripole array can avoid the ambiguity problem, it means that for nonlinearly polarised signals if $\alpha_1 \neq \alpha_2$, the joint steering vectors $\boldsymbol{v}_1$ and $\boldsymbol{v}_1$ will never be in parallel with each other.

To prove these two statements, firstly we give the following definition and lemma.

Definition. *Given two signals from distinct directions* (θ_1, ϕ_1) *and* (θ_2, ϕ_2)*, the two signals are in DOA parallel if* $\mathbf{a}_1 = \mathbf{a}_2$.

Equation (1) indicates that $\boldsymbol{a}$ is only determined by the value of $\sin\theta\sin\phi$. If it satisfies

$$\sin\theta_1\sin\phi_1 = \sin\theta_2\sin\phi_2 \tag{14}$$

the two steering vectors will be the same, i.e. $\boldsymbol{a}_1 = \boldsymbol{a}_2$. In the upper hemisphere space ($0 \le \theta \le \pi/2$, $0 \le \phi \le 2\pi$), there are infinite number of directions in DOA parallel with a given direction.

Lemma. *Given two complex-valued vectors* $\mathbf{w}_1 = \mathbf{a}_1 \otimes \mathbf{q}_1$ *and* $\mathbf{w}_2 = \mathbf{a}_2 \otimes \mathbf{q}_2$, $\mathbf{w}_1 // \mathbf{w}_2$ *is necessary and sufficient for* $\mathbf{a}_1 // \mathbf{a}_2$ *and* $\mathbf{q}_1 // \mathbf{q}_2$.

The proof can be found in Appendix A. Although we used the joint steering vector of the crossed-dipole array in the proof, it is straightforward to show that the lemma is also applicable to the joint steering vector of tripole sensor arrays.

Now we first consider the ambiguity problem in crossed-dipole sensor arrays. Given $\boldsymbol{w}_1 = \boldsymbol{a}_1 \otimes \boldsymbol{q}_1$, our aim is to find a vector $\boldsymbol{w}_2 = \boldsymbol{a}_2 \otimes \boldsymbol{q}_2$ with $\boldsymbol{a}_1 // \boldsymbol{a}_2$ and $\boldsymbol{q}_1 // \boldsymbol{q}_2$ when $\alpha_1 \neq \alpha_2$.

As mentioned in the DOA parallel definition, any direction that satisfies (14) has the steering vector $\boldsymbol{a}_2 // \boldsymbol{a}_1$. With the constraints, we need further choose values for γ_2 and η_2 to satisfy $\boldsymbol{q}_1 // \boldsymbol{q}_2$. From (6) and (11), the polarisation vector $\boldsymbol{q}_1$ is determined by all four parameters θ_1, ϕ_1, γ_1 and η_1, where

$$\boldsymbol{q}_1 = \begin{bmatrix} \cos\theta_1\cos\phi_1 & -\sin\phi_1 \\ \cos\theta_1\sin\phi_1 & \cos\phi_1 \end{bmatrix} \begin{bmatrix} \sin\gamma_1 e^{j\eta_1} \\ \cos\gamma_1 \end{bmatrix} = \boldsymbol{\Psi}_1 \boldsymbol{g}_1 \tag{15}$$

Hence, the other polarisation vector $\boldsymbol{q}_2 = \boldsymbol{\Psi}_2 \boldsymbol{g}_2$ needs to satisfy

$$\boldsymbol{\Psi}_1 \boldsymbol{g}_1 = \lambda \boldsymbol{\Psi}_2 \boldsymbol{g}_2 \;\Rightarrow\; \boldsymbol{g}_2 = \lambda^{-1} \boldsymbol{\Psi}_2^{-1} \boldsymbol{\Psi}_1 \boldsymbol{g}_1 \tag{16}$$

λ is a constant and without loss of generality we assume its value is 1. Here $\boldsymbol{g}_2$ is a 2×1 vector with $\boldsymbol{g}_2[1] = \sin\gamma_2 e^{j\eta_2}$ and $\boldsymbol{g}_2[2] = \cos\gamma_2$, where "[1]" and "[2]" denote the first and the second elements of the vector.

$$\tan\gamma_2 = \frac{|\boldsymbol{g}_2[1]|}{|\boldsymbol{g}_2[2]|} \qquad \tan\eta_2 = \frac{\mathrm{Im}\{\boldsymbol{g}_2[1]/\boldsymbol{g}_2[2]\}}{\mathrm{Re}\{\boldsymbol{g}_2[1]/\boldsymbol{g}_2[2]\}} \tag{17}$$

The new parameters from (14) ensure $\boldsymbol{a}_1 // \boldsymbol{a}_2$ and the new parameters from (17) ensure $\boldsymbol{q}_1 // \boldsymbol{q}_2$ with the constraint $\alpha_1 \neq \alpha_2$. After that, the new joint steering vector $\boldsymbol{w}_2$ will be in parallel with the original $\boldsymbol{w}_1$. As a result, we can not uniquely determine the four DOA and polarisation parameters of a source using the crossed-dipole array.

Next, we consider the tripole sensor array case. Given a joint steering vector $\boldsymbol{v}_1 = \boldsymbol{a}_1 \otimes \boldsymbol{p}_1$, we want to prove that a parallel $\boldsymbol{v}_2 = \boldsymbol{a}_2 \otimes \boldsymbol{p}_2$ does not exist and we prove it by contradiction.

Similar to the crossed-dipole case, firstly a new direction which is in DOA parallel to the original direction is selected so that the new elevation and azimuth angles ensure $\boldsymbol{a}_1 // \boldsymbol{a}_2$. This step is clearly feasible and the new direction can be obtained by (14). The remaining part of the problem is that whether there exists another polarisation vector $\boldsymbol{p}_2$ which is in parallel with $\boldsymbol{p}_1$. Assuming that $\boldsymbol{p}_2$ exists, i.e.

$$\boldsymbol{\Omega}_1 \boldsymbol{g}_1 = \lambda \boldsymbol{\Omega}_2 \boldsymbol{g}_2 \tag{18}$$

where λ is an unknown complex-valued constant. Expanding $\boldsymbol{\Omega}_1$ and $\boldsymbol{\Omega}_2$ by the column vector, where $\boldsymbol{\Omega}_{11}$ and $\boldsymbol{\Omega}_{12}$ are the first and second column vectors of $\boldsymbol{\Omega}_1$, and $\boldsymbol{\Omega}_{21}$ and $\boldsymbol{\Omega}_{22}$ are the first and second column vectors of $\boldsymbol{\Omega}_2$, respectively. (18) is transformed to

$$[\boldsymbol{\Omega}_{11} \quad \boldsymbol{\Omega}_{12}] \begin{bmatrix} \boldsymbol{g}_1[1] \\ \boldsymbol{g}_1[2] \end{bmatrix} = \lambda [\boldsymbol{\Omega}_{21} \quad \boldsymbol{\Omega}_{22}] \begin{bmatrix} \boldsymbol{g}_2[1] \\ \boldsymbol{g}_2[2] \end{bmatrix} \;\Leftrightarrow$$

$$\boldsymbol{\Omega}_{11} \boldsymbol{g}_1[1] + \boldsymbol{\Omega}_{12} \boldsymbol{g}_1[2] = \boldsymbol{\Omega}_{21} \boldsymbol{g}_2[1]\lambda + \boldsymbol{\Omega}_{22} \boldsymbol{g}_2[2]\lambda \tag{19}$$

The left side of (19) can be viewed as a vector which is a linear combination of $\boldsymbol{\Omega}_{11}$ and $\boldsymbol{\Omega}_{12}$. The right is a linear combination of $\boldsymbol{\Omega}_{21}$ and $\boldsymbol{\Omega}_{22}$. Here we define a 2-D space $\boldsymbol{A}_1$ spanned by $\boldsymbol{\Omega}_{11}$ and $\boldsymbol{\Omega}_{12}$, also $\boldsymbol{A}_2$ spanned by $\boldsymbol{\Omega}_{21}$ and $\boldsymbol{\Omega}_{22}$. Since $\boldsymbol{\Omega}_{11}, \boldsymbol{\Omega}_{12}, \boldsymbol{\Omega}_{21}$ and $\boldsymbol{\Omega}_{22}$ are all 3×1 vectors, the equation holds only in the following two cases:

Case 1: $\boldsymbol{A}_1$ and $\boldsymbol{A}_2$ are the same 2-D span.

It can be noticed that $\boldsymbol{A}_1$ intersects with the $x - y$ plane at vector $\boldsymbol{\Omega}_{12}$, and $\boldsymbol{A}_2$ intersects with the $x - y$ plane at vector $\boldsymbol{\Omega}_{22}$. If $\boldsymbol{A}_1$ and $\boldsymbol{A}_2$ are the same 2-D span, it must satisfy $\boldsymbol{\Omega}_{12} // \boldsymbol{\Omega}_{22}$, and then we have

$$\begin{bmatrix} -\sin\phi_1 \\ \cos\phi_1 \\ 0 \end{bmatrix} // \begin{bmatrix} -\sin\phi_2 \\ \cos\phi_2 \\ 0 \end{bmatrix} \Leftrightarrow -\frac{\sin\phi_1}{\cos\phi_1} = -\frac{\sin\phi_2}{\cos\phi_2}$$

$$\Leftrightarrow \tan\phi_1 = \tan\phi_2 \tag{20}$$

However, $\phi_1 \neq \phi_2$ and (20) contradicts with the basic assumption, which means that with the tripole sensor array, there is no other joint steering vector $\boldsymbol{v}_2$ in parallel with the given $\boldsymbol{v}_1$ in such a case.

Case 2: $\boldsymbol{A}_1$ and $\boldsymbol{A}_2$ are two different 2-D spans. Then $\boldsymbol{p}_1$ and $\boldsymbol{p}_2$ must be in parallel with the intersecting vector of $\boldsymbol{A}_1$ and $\boldsymbol{A}_2$. Firstly, we denote the intersecting vector as $\boldsymbol{\Omega}_x$. Since $\boldsymbol{\Omega}_{11}, \boldsymbol{\Omega}_{12}, \boldsymbol{\Omega}_{21}, \boldsymbol{\Omega}_{22}$ are all real-valued, all the elements in $\boldsymbol{\Omega}_x$ must also be real-valued. From eq.(5), $\boldsymbol{p}_1$ can be transformed to

$$\boldsymbol{p}_1 = e^{j\eta} \begin{bmatrix} \cos\theta\cos\phi\sin\gamma - \sin\phi\cos\gamma e^{-j\eta} \\ \cos\theta\sin\phi\sin\gamma + \cos\phi\cos\gamma e^{-j\eta} \\ -\sin\theta\sin\gamma \end{bmatrix} = e^{j\eta} \cdot \hat{\boldsymbol{p}}_1 \tag{21}$$

It can be seen that $\boldsymbol{p}_1 // \hat{\boldsymbol{p}}_1$. In most situations, with $\gamma \neq 90^\circ$, $\gamma \neq 0$ and $\eta \neq 0$ (nonlinearly polarized), the first two elements in $\hat{\boldsymbol{p}}_1$ are complex-valued and the last element in $\hat{\boldsymbol{p}}_1$ is real-valued, which indicates that with such a situation, it is impossible for $\hat{\boldsymbol{p}}_1$ to be in parallel with the intersecting vector $\boldsymbol{\Omega}_x$. Hence, if the incoming signal is nonlinearly polarised, there is no ambiguity in joint estimation with tripole sensors.

C. Ambiguity with Linearly Polarised Signals

If the signals are linearly polarised, $\gamma = 90^\circ$ or $\gamma = 0$ or $\eta = 0$. $\hat{\boldsymbol{p}}_1$ or $\boldsymbol{p}_1$ becomes a real-valued vector, and it may be possible for $\boldsymbol{p}_1$ to be in parallel with the intersecting vector $\boldsymbol{\Omega}_x$. Now with the assumption $\boldsymbol{p}_1 // \boldsymbol{p}_2 // \boldsymbol{\Omega}_x$, $\boldsymbol{p}_1$ and $\boldsymbol{p}_2$ must all be real-valued, which means $\gamma_1 = 90^\circ$ or $\gamma_1 = 0$ or $\eta_1 = 0$, and at the same time $\gamma_2 = 90^\circ$ or $\gamma_2 = 0$ or $\eta_2 = 0$. With the constraint $\sin\theta_1\sin\phi_1 = \sin\theta_2\sin\phi_2$, we consider all of the following cases:

Case 1: $\gamma_1 = 90°$ and $\gamma_2 = 90°$.

$$\boldsymbol{p}_1 = e^{j\eta_1}\begin{bmatrix}\cos\theta_1\cos\phi_1\\ \cos\theta_1\sin\phi_1\\ -\sin\theta_1\end{bmatrix} \qquad \boldsymbol{p}_2 = e^{j\eta_2}\begin{bmatrix}\cos\theta_2\cos\phi_2\\ \cos\theta_2\sin\phi_2\\ -\sin\theta_2\end{bmatrix} \tag{22}$$

With $\theta_1 = \theta_2$ and $\phi_1 = \phi_2$, we have $\boldsymbol{p}_1 // \boldsymbol{p}_2$ for arbitrary η_1 and η_2. An example is $(30°, 60°, 90°, 20°)$ and $(30°, 60°, 90°, 50°)$.

Case 2: $\gamma_1 = 90°$ and $\gamma_2 = 0°$. (same for $\gamma_1 = 0°$ and $\gamma_2 = 90°$)

$$\boldsymbol{p}_1 = e^{j\eta_1}\begin{bmatrix}\cos\theta_1\cos\phi_1\\ \cos\theta_1\sin\phi_1\\ -\sin\theta_1\end{bmatrix} \qquad \boldsymbol{p}_2 = \begin{bmatrix}-\sin\phi_2\\ \cos\phi_2\\ 0\end{bmatrix} \tag{23}$$

In this case, with $\theta_1 = 0°$ and $\tan\phi_1 = -\cot\phi_2$, we have $\boldsymbol{p}_1 // \boldsymbol{p}_2$ for arbitrary θ_2, η_1 and η_2. An example is $(0°, 90°, 90°, 20°)$ and $(50°, 0°, 0°, 50°)$.

Case 3: $\gamma_1 = 90°$ and $\eta_2 = 0°$. (same for $\eta_1 = 0°$ and $\gamma_2 = 90°$)

$$\boldsymbol{p}_1 = e^{j\eta_1}\begin{bmatrix}\cos\theta_1\cos\phi_1\\ \cos\theta_1\sin\phi_1\\ -\sin\theta_1\end{bmatrix}$$
$$\boldsymbol{p}_2 = \begin{bmatrix}\cos\theta_2\cos\phi_2\sin\gamma_2 - \sin\phi_2\cos\gamma_2\\ \cos\theta_2\sin\phi_2\sin\gamma_2 + \cos\phi_2\cos\gamma_2\\ -\sin\theta_2\sin\gamma_2\end{bmatrix} \tag{24}$$

Given arbitrary $\theta_1, \phi_1, \theta_2, \phi_2$ which satisfy the constraint (14), if $\boldsymbol{p}_1 // \boldsymbol{p}_2$, then

$$\begin{cases}\dfrac{\sin\theta_1}{\sin\theta_2\sin\gamma_2} = \dfrac{\cos\theta_1\cos\phi_1}{\cos\theta_2\cos\phi_2\sin\gamma_2 - \sin\phi_2\cos\gamma_2}\\ \dfrac{\sin\theta_1}{\sin\theta_2\sin\gamma_2} = \dfrac{\cos\theta_1\sin\phi_1}{\cos\theta_2\sin\phi_2\sin\gamma_2 + \cos\phi_2\cos\gamma_2}\end{cases} \tag{25}$$

leading to

$$\begin{cases}\sin\phi_2 = \cos\phi_2\\ \sin\phi_2 = -\cos\phi_2\end{cases} \tag{26}$$

which causes contradiction. In this case, there is no ambiguity.

Case 4: $\gamma_1 = 0°$ and $\gamma_2 = 0°$.

$$\boldsymbol{p}_1 = \begin{bmatrix}-\sin\phi_1\\ \cos\phi_1\\ 0\end{bmatrix} \qquad \boldsymbol{p}_2 = \begin{bmatrix}-\sin\phi_2\\ \cos\phi_2\\ 0\end{bmatrix} \tag{27}$$

In this case, with $\phi_1 = \phi_2$, we have $\boldsymbol{p}_1 // \boldsymbol{p}_2$ for arbitrary η_1 and η_2. An example is $(30°, 60°, 0°, 20°)$ and $(30°, 60°, 0°, 50°)$.

Case 5: $\gamma_1 = 0°$ and $\eta_2 = 0°$. (same for $\eta_1 = 0°$ and $\gamma_2 = 0°$)

$$\boldsymbol{p}_1 = \begin{bmatrix}-\sin\phi_1\\ \cos\phi_1\\ 0\end{bmatrix}$$
$$\boldsymbol{p}_2 = \begin{bmatrix}\cos\theta_2\cos\phi_2\sin\gamma_2 - \sin\phi_2\cos\gamma_2\\ \cos\theta_2\sin\phi_2\sin\gamma_2 + \cos\phi_2\cos\gamma_2\\ -\sin\theta_2\sin\gamma_2\end{bmatrix} \tag{28}$$

In this case, to satisfy the parallel condition, firstly θ_2 should be $0°$ and η_1 can be an arbitrary value. Further we have

$$\tan\gamma_2 = \frac{\cos\phi_1\sin\phi_2 - \sin\phi_1\cos\phi_2}{\cos\phi_1\cos\phi_2 + \sin\phi_1\sin\phi_2} \tag{29}$$

An example is $(30°, 0°, 0°, 30°)$ and $(0°, 30°, 30°, 0°)$.

Case 6: $\eta_1 = 0°$ and $\eta_2 = 0°$.

$$\boldsymbol{p}_1 = \begin{bmatrix}\cos\theta_1\cos\phi_1\sin\gamma_1 - \sin\phi_1\cos\gamma_1\\ \cos\theta_1\sin\phi_1\sin\gamma_1 + \cos\phi_1\cos\gamma_1\\ -\sin\theta_1\sin\gamma_1\end{bmatrix}$$
$$\boldsymbol{p}_2 = \begin{bmatrix}\cos\theta_2\cos\phi_2\sin\gamma_2 - \sin\phi_2\cos\gamma_2\\ \cos\theta_2\sin\phi_2\sin\gamma_2 + \cos\phi_2\cos\gamma_2\\ -\sin\theta_2\sin\gamma_2\end{bmatrix} \tag{30}$$

In this case, due to the parallel condition, we know

$$\begin{cases}\dfrac{\sin\theta_1\sin\gamma_1}{\sin\theta_2\sin\gamma_2} = \dfrac{\cos\theta_1\cos\phi_1\sin\gamma_1 - \sin\phi_1\cos\gamma_1}{\cos\theta_2\cos\phi_2\sin\gamma_2 - \sin\phi_2\cos\gamma_2}\\ \dfrac{\sin\theta_1\sin\gamma_1}{\sin\theta_2\sin\gamma_2} = \dfrac{\cos\theta_1\sin\phi_1\sin\gamma_1 + \cos\phi_1\cos\gamma_1}{\cos\theta_2\sin\phi_2\sin\gamma_2 + \cos\phi_2\cos\gamma_2}\end{cases} \tag{31}$$

Each equations in (31) will produce a unique solution to $\tan\gamma_2$. Except that all the parameters $(\theta_1, \phi_1, \gamma_1) = (\theta_2, \phi_2, \gamma_2)$, there is no other solutions for γ_2 and therefore there is no ambiguity in this case.

Table I gives a summary of the ambiguity problem between array and signal types, where '✗' means there is ambiguity in the estimation while with '✓' no ambiguity exists.

TABLE I
AMBIGUITY BETWEEN ARRAY AND SIGNAL TYPES

Array type \ Signal	Non-linearly polarised	Linearly polarised (Case:1,2,4,5)	Linearly polarised (Case:3,6)
Crossed-dipole	✗	✗	✗
Tripole	✓	✗	✓

III. Simulation Results

In this section, simulation results are presented to demonstrate the ambiguity issues discussed earlier and the performance of the proposed linear tripole arrays.

A. Ambiguity for Non-Linearly Polarised Signals

Assuming one source signal from $(\theta, \phi, \gamma, \eta) = (30°, 80°, 20°, 50°)$ impinges on both arrays. Both have the same senor number $N = 5$ and $d = \lambda/2$. SNR is 10 dB. A 2-D estimator is used to estimate the DOA and polarisations [36]. The 2-D estimator divides the 4-D estimation into two separate 2-D searches, i.e. the 2-D DOA and the 2-D polarisation search. Here we only focus on the DOA estimation by the 2-D estimator.

Figs. 2(a) and 2(b) present the DOA estimation results for these two arrays, respectively. Apparently, the tripole array gives a unique peak at the source direction while the crossed-dipole array shows a peak line due to the ambiguity problem and there is no way to identify the real direction of the signal.

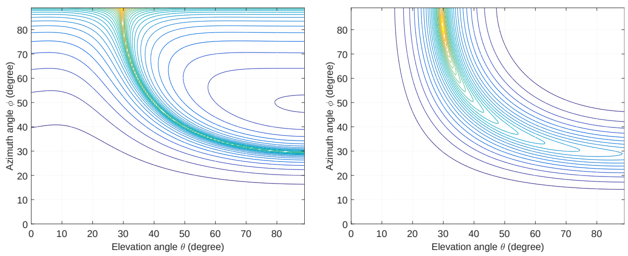

(a) Linear crossed-dipole array. (b) Linear tripole array

Fig. 2. DOA spectrum of non-linearly polarised signal (top contour view).

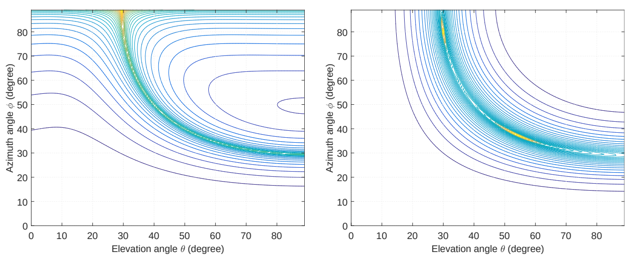

(a) Linear crossed-dipole array. (b) Linear tripole array

Fig. 3. DOA spectrum of linearly polarised signal (top contour view).

B. Ambiguity for Linearly Polarised Signals

Consider a linearly polarised signal from $(\theta, \phi, \gamma, \eta) = (30°, 80°, 20°, 0°)$. The array is constructed with $N = 5$ sensors with $d = 0.3\lambda$ and the SNR is 10 dB. The 2-D estimator is applied to provide the DOA estimation spectrums, which are shown in Figs. 3(a) and 3(b). The spectrum of Fig. 3(a) by crossed-dipole array is very similar to the results for non-linearly polarised signals in Fig. 2(a) where there are infinite number of ambiguity directions along a peak line satisfying $\sin\theta \sin\phi = \sin 30° \sin 80°$. However, the spectrum of Fig. 3(b) indicates that the ambiguity still exists with the tripole array. However, the ambiguity direction is no more of an infinite number, and there is only one ambiguity direction at $(\theta, \phi) = (53°, 38°)$.

C. RMSE Results

Now we study the performance of tripole arrays for DOA and polarisation estimation. Consider two signals from $(\theta, \phi, \gamma, \eta) = (10°, 20°, 15°, 30°)$ and $(\theta, \phi, \gamma, \eta) = (60°, 70°, 60°, 80°)$. The tripole sensor number is $N = 4$ and the number of snapshots is $K = 1000$. Firstly, we compare the estimation results in two cases. The first case is that the two sources are uncorrelated while the second case is that the two sources are partially correlated with correlation coefficient $\rho = 0.71$. After applying the 2-D estimator, the results for θ and γ are shown in Figs. 4(a)-4(b), respectively, where we can see that uncorrelated sources has a smaller error than partially correlated ones. With the increase of SNR, the estimation accuracy of the two cases also increases. The results for ϕ and η are omitted as they show a similar trend.

Now we compare the performance of the 4-D estimator [36], the 2-D estimator [36], [37], 2-D estimator with Newton optimization (see Appendix B) and the CRB for uncorrelated sources. The RMSE results are shown in Figs. 5(a)-5(d), where

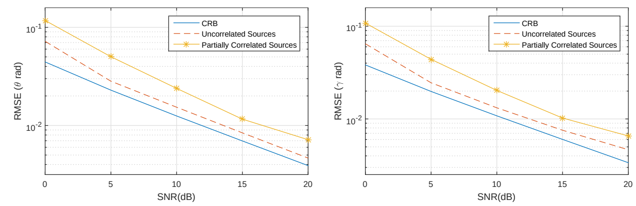

(a) RMSE of θ. (b) RMSE of γ.

Fig. 4. Uncorrelated sources versus partially correlated sources.

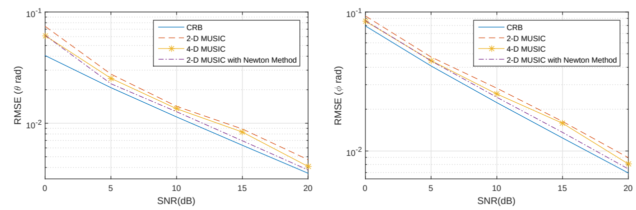

(a) RMSE of θ. (b) RMSE of ϕ.

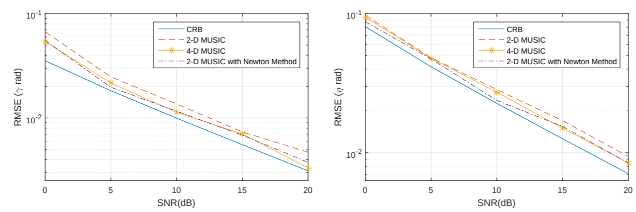

(c) RMSE of γ. (d) RMSE of η.

Fig. 5. RMSE of uncorrelated sources.

we can see that with the increase of SNR, the RMSE level decreases consistently, and the accuracy of the 4-D MUSIC is always better than the 2-D estimator. However, after Newton optimization, the 2-D estimator has achieved an even higher accuracy, very close to the CRB [37], with a complexity still much lower than the 4-D estimator.

D. Linear Tripole and Planar Crossed-dipole Arrays

Since a planar crossed-dipole array can also be used to estimate the four parameters, it would be interesting to know that given the same number of dipoles, which one is more effective for 4-D parameter estimation, the linear tripole array or the planar crossed-dipole array. Consider a 4×1 linear tripole array and a 2×3 planar crossed-dipole array with the same number of dipoles or DOFs. We compare their estimation accuracy using the 2-D MUSIC algorithm [36]. All the other conditions are the same as in Section III-C.

Fig. 6 shows the RMSE results for the first signal's azimuth angle. It can be seen that the planar array has given a higher estimating accuracy and its CRB is much lower than the linear tripole array, which means that the compact structure of the linear tripole array is achieved at the cost of estimation accuracy.

IV. Conclusion and Discussion

With a detailed analysis and proof, it has been shown that due to inherent limitation of the linear crossed-dipole structure, it cannot uniquely identify the four parameters associated with

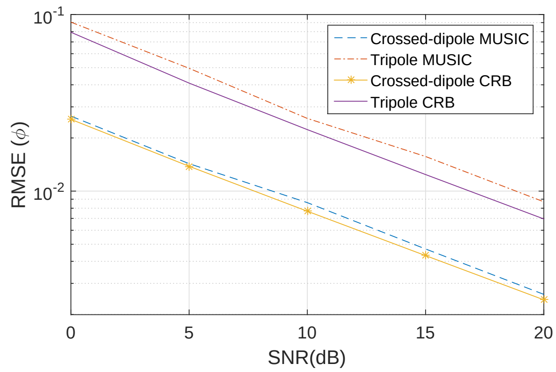

Fig. 6. RMSE of crossed-dipole and tripole sensor arrays.

impinging signals. In order to simultaneously estimate both the 2-D DOA and 2-D polarisation parameters of the impinging signals, we could increase the dimension of the array and construct a planar crossed-dipole array. To avoid this and have a compact structure, a linear tripole array has been employed instead. It has been proved and also shown that such a structure can estimate the 2-D DOA and 2-D polarisation information effectively except for some very special cases. Finally, a brief comparison has shown that given the same number of dipoles, the planar structure has a better performance, although this is achieved at the cost of increased physical size.

Appendix A
Proof of the Lemma

Necessity: If $\boldsymbol{a}_1//\boldsymbol{a}_2$ and $\boldsymbol{q}_1//\boldsymbol{q}_2$, then

$$\boldsymbol{a}_2 = k_1 \cdot \boldsymbol{a}_1 \qquad \boldsymbol{q}_2 = k_2 \cdot \boldsymbol{q}_1 \tag{32}$$

where k_1 and k_2 are arbitrary complex-valued constants. Then,

$$\begin{aligned}\boldsymbol{w}_2 &= \boldsymbol{a}_2 \otimes \boldsymbol{q}_2 = (k_1 \cdot \boldsymbol{a}_1) \otimes (k_2 \cdot \boldsymbol{q}_1) \\ &= (k_1 k_2) \cdot (\boldsymbol{a}_1 \otimes \boldsymbol{q}_1) = (k_1 k_2) \cdot \boldsymbol{w}_1\end{aligned} \tag{33}$$

Hence, $\boldsymbol{w}_1//\boldsymbol{w}_2$.

Sufficiency: By (10), $\boldsymbol{w}$ can be expanded as

$$\boldsymbol{w} = \boldsymbol{a} \otimes \boldsymbol{q} = \begin{bmatrix} a_1\boldsymbol{q} \\ \cdot \\ \cdot \\ \cdot \\ a_N\boldsymbol{q} \end{bmatrix} = \begin{bmatrix} a_1 p_x \\ a_1 p_y \\ \cdot \\ \cdot \\ \cdot \\ a_N p_x \\ a_N p_y \end{bmatrix} \tag{34}$$

The Hermitian transpose $\boldsymbol{w}^H$ is given by

$$\boldsymbol{w}^H = \boldsymbol{a}^H \otimes \boldsymbol{q}^H \tag{35}$$

The norm of $\boldsymbol{w}$ is

$$\begin{aligned}|\boldsymbol{w}| &= \sqrt{\boldsymbol{w}^H\boldsymbol{w}} = \sqrt{(a_1 a_1^* + \ldots + a_N a_N^*)(p_x p_x^* + p_y p_y^*)} \\ &= |\boldsymbol{a}| \cdot |\boldsymbol{q}|\end{aligned} \tag{36}$$

Then, we have

$$|\boldsymbol{w}_1| = |\boldsymbol{a}_1| \cdot |\boldsymbol{q}_1| \qquad |\boldsymbol{w}_2| = |\boldsymbol{a}_2| \cdot |\boldsymbol{q}_2| \tag{37}$$

Generally, by (35), the modulus of the inner product of $\boldsymbol{w}_1$ and $\boldsymbol{w}_2$ can be expanded as

$$|\boldsymbol{w}_1^H \boldsymbol{w}_2| = |(\boldsymbol{a}_1^H \otimes \boldsymbol{q}_1^H) \cdot (\boldsymbol{a}_2 \otimes \boldsymbol{q}_2)| \tag{38}$$

According to the mixed-product property of Kronecker product, lemma 4.2.10 in [49], (38) can be deduced to

$$\begin{aligned}|\boldsymbol{w}_1^H \boldsymbol{w}_2| &= |\boldsymbol{a}_1^H \cdot \boldsymbol{a}_2| \otimes |\boldsymbol{q}_1^H \cdot \boldsymbol{q}_2| \\ &\leq |\boldsymbol{a}_1| \cdot |\boldsymbol{a}_2| \cdot |\boldsymbol{q}_1| \cdot |\boldsymbol{q}_2|\end{aligned} \tag{39}$$

On the other hand, since $\boldsymbol{w}_1//\boldsymbol{w}_2$, we know $\boldsymbol{w}_2 = k\boldsymbol{w}_1$ and $|\boldsymbol{w}_2| = |k||\boldsymbol{w}_1|$, which leads to

$$\begin{aligned}|\boldsymbol{w}_1^H \boldsymbol{w}_2| &= |\boldsymbol{w}_1^H \cdot k\boldsymbol{w}_1| = |k||\boldsymbol{w}_1| \cdot |\boldsymbol{w}_1| \\ &= |\boldsymbol{w}_1| \cdot |\boldsymbol{w}_2| = |\boldsymbol{a}_1| \cdot |\boldsymbol{a}_2| \cdot |\boldsymbol{q}_1| \cdot |\boldsymbol{q}_2|\end{aligned} \tag{40}$$

The equality in (39) holds only when $\boldsymbol{a}_1//\boldsymbol{a}_2$ and $\boldsymbol{q}_1//\boldsymbol{q}_2$. Combined with (40), the sufficiency proof is completed.

Appendix B
2-D Estimator with Newton Method

As introduced in [36], [37], the 2-D MUSIC estimator includes the following steps: Firstly, the noise subspace is derived by applying eigenvalue decomposition to $\hat{\boldsymbol{R}}$. The lase $3N-M$ (N is the sensor number and M is the signal number) eigenvalues and the corresponding eigenvectors form the noise space $\boldsymbol{U}_n$. After that, apply the following 2-D estimator to find θ and ϕ,

$$f(\theta, \phi) = \frac{det\{\boldsymbol{B}^H\boldsymbol{B}\}}{det\{\boldsymbol{B}^H\boldsymbol{U}_n\boldsymbol{U}_n^H\boldsymbol{B}\}} \tag{41}$$

where $\boldsymbol{B}$ is the steering matrix associated with θ and ϕ (see (13) in [36]). After obtaining θ and ϕ, the polarisation γ and η can be estimated by the following estimator through another 2-D search:

$$f(\gamma, \eta) = \frac{\boldsymbol{g}^H\boldsymbol{B}^H\boldsymbol{B}\boldsymbol{g}}{\boldsymbol{g}^H\boldsymbol{B}^H\boldsymbol{U}_n\boldsymbol{U}_n^H\boldsymbol{B}\boldsymbol{g}} \tag{42}$$

where $\boldsymbol{g} = [\cos\gamma \quad \sin\gamma e^{j\eta}]^T$ is the polarisation vector.

The estimates of θ and ϕ can be further refined by the Newton method. In the spectrum, the peak directions satisfy $det\{\boldsymbol{B}^H\boldsymbol{U}_n\boldsymbol{U}_n^H\boldsymbol{B}\} = 0$. Define

$$l(\theta, \phi) = det\{\boldsymbol{B}^H\boldsymbol{U}_n\boldsymbol{U}_n^H\boldsymbol{B}\} \tag{43}$$

It can be verified that $l(\theta, \phi)$ is non-negative valued. When θ and ϕ meet the source signals' direction, $l(\theta, \phi)$ will reach a minimum value, where

$$\nabla_l(\theta, \phi) = 0 \Rightarrow \begin{cases} \dfrac{\partial l(\theta, \phi)}{\partial \theta} = 0 \\ \dfrac{\partial l(\theta, \phi)}{\partial \phi} = 0 \end{cases} \tag{44}$$

where ∇ denotes the gradient of $l(\theta, \phi)$.

With a rough estimation of θ_a, ϕ_a provided by the 2-D estimator, the partial derivative with regard to θ_a is possibly not equal to 0. If a tangent is plotted through (θ_a, ϕ_a) along the θ-axis direction of $\frac{\partial l(\theta,\phi)}{\partial \theta}$, the equation can be denoted as

$$l_2(\theta, \phi) = \frac{\partial^2 l(\theta_a, \phi_a)}{\partial \theta^2}(\theta - \theta_a) + l(\theta_a, \phi_a) \tag{45}$$

Then the intersection between the equation and the θ-axis should be

$$0 = \frac{\partial^2 l(\theta_a, \phi_a)}{\partial \theta^2}(\theta_b - \theta_a) + \frac{\partial l(\theta_a, \phi_a)}{\partial \theta} \tag{46}$$

The Newton method provides a more accurate value θ_b than θ_a with one trial, where

$$\theta_b = \theta_a - \frac{\partial l(\theta_a, \phi_a)}{\partial \theta} / \frac{\partial^2 l(\theta_a, \phi_a)}{\partial \theta^2} \tag{47}$$

Similarly, the other parameter ϕ can be approached by

$$\phi_b = \phi_a - \frac{\partial l(\theta_a, \phi_a)}{\partial \phi} / \frac{\partial^2 l(\theta_a, \phi_a)}{\partial \phi^2} \tag{48}$$

The above process should be repeated in a finite number of trials to obtain a better result.

REFERENCES

[1] A. Nehorai and E. Paldi, "Vector-sensor array processing for electromagnetic source localization," *IEEE Transactions on Signal Processing*, vol. 42, no. 2, pp. 376–398, 1994.

[2] S. Liu, M. Jin, and X. Qiao, "Joint polarization-DOA estimation using circle array," in *Proc. IET International Radar Conference*, 2009, pp. 1–5.

[3] X. Lan and W. Liu, "Fully quaternion-valued adaptive beamforming based on crossed-dipole arrays," *Electronics*, vol. 6, no. 2, p. 34, 2017.

[4] X. Yuan, K. T. Wong, Z. Xu, and K. Agrawal, "Various compositions to form a triad of collocated dipoles/loops, for direction finding and polarization estimation," *IEEE Sensors Journal*, vol. 12, no. 6, pp. 1763–1771, 2012.

[5] X. R. Zhang, Z. W. Liu, W. Liu, and Y. G. Xu, "Quasi-vector-cross-product based direction finding algorithm with a spatially stretched tripole," in *Proc. the IEEE TENCON Conference*, Xi'an, China, October 2013.

[6] P. Chevalier, A. Ferréol, L. Albera, and G. Birot, "Higher order direction finding from arrays with diversely polarized antennas: The PD-2q-MUSIC algorithms," *IEEE Transactions on Signal Processing*, vol. 55, no. 11, pp. 5337–5350, 2007.

[7] B. Friedlander and A. J. Weiss, "Performance of diversely polarized antenna arrays for correlated signals," *IEEE Transactions on Aerospace and Electronic Systems*, vol. 28, no. 3, pp. 869–879, 1992.

[8] K. T. Wong, "Direction finding/polarization estimation-dipole and/or loop triad (s)," *IEEE Transactions on Aerospace and Electronic Systems*, vol. 37, no. 2, pp. 679–684, 2001.

[9] Y. Xu and Z. Liu, "Simultaneous estimation of 2-D DOA and polarization of multiple coherent sources using an electromagnetic vector sensor array," *Journal-China Institute of Communications*, vol. 25, no. 5, pp. 28–38, 2004.

[10] M. D. Zoltowski and K. T. Wong, "ESPRIT-based 2-D direction finding with a sparse uniform array of electromagnetic vector sensors," *IEEE Transactions on Signal Processing*, vol. 48, no. 8, pp. 2195–2204, 2000.

[11] E. Ferrara and T. Parks, "Direction finding with an array of antennas having diverse polarizations," *IEEE Transactions on Antennas and Propagation*, vol. 31, no. 2, pp. 231–236, 1983.

[12] B. Friedlander and A. J. Weiss, "The resolution threshold of a direction-finding algorithm for diversely polarized arrays," *IEEE Transactions on Signal Processing*, vol. 42, no. 7, pp. 1719–1727, 1994.

[13] H. Lee and R. Stovall, "Maximum likelihood methods for determining the direction of arrival for a single electromagnetic source with unknown polarization," *IEEE Transactions on Signal Processing*, vol. 42, no. 2, pp. 474–479, 1994.

[14] M. D. Jiang, Y. Li, and W. Liu, "Properties of a general quaternion-valued gradient operator and its application to signal processing," *Frontiers of Information Technology & Electronic Engineering*, vol. 17, pp. 83–95, February 2016.

[15] F. Li, H. Liu, and R. J. Vaccaro, "Performance analysis for doa estimation algorithms: unification, simplification, and observations," *IEEE Transactions on Aerospace and Electronic Systems*, vol. 29, no. 4, pp. 1170–1184, 1993.

[16] Z. Ye, J. Dai, X. Xu, and X. Wu, "DOA estimation for uniform linear array with mutual coupling," *IEEE Transactions on Aerospace and Electronic Systems*, vol. 45, no. 1, pp. 280–288, 2009.

[17] J. A. Cadzow, Y.-S. Kim, and D.-C. Shiue, "General direction-of-arrival estimation: a signal subspace approach," *IEEE Transactions on Aerospace and Electronic Systems*, vol. 25, no. 1, pp. 31–47, 1989.

[18] M. Wax and T. Kailath, "Detection of signals by information theoretic criteria," *IEEE Transactions on acoustics, speech, and signal processing*, vol. 33, no. 2, pp. 387–392, 1985.

[19] J. He, M. O. Ahmad, and M. Swamy, "Near-field localization of partially polarized sources with a cross-dipole array," *IEEE Transactions on Aerospace and Electronic Systems*, vol. 49, no. 2, pp. 857–870, 2013.

[20] M. Hurtado and A. Nehorai, "Performance analysis of passive low-grazing-angle source localization in maritime environments using vector sensors," *IEEE Transactions on Aerospace and Electronic Systems*, vol. 43, no. 2, pp. 780–789, 2007.

[21] J. Li and R. Compton, "Angle and polarization estimation in a coherent signal environment," *IEEE transactions on aerospace and electronic systems*, vol. 29, no. 3, pp. 706–716, 1993.

[22] R. O. Schmidt, "Multiple emitter location and signal parameter estimation," *IEEE Transactions on Antennas and Propagation*, vol. 34, no. 3, pp. 276–280, March 1986.

[23] S. Miron, N. Le Bihan, and J. I. Mars, "Quaternion-MUSIC for vector-sensor array processing," *IEEE Transactions on Signal Processing*, vol. 54, no. 4, pp. 1218–1229, April 2006.

[24] X. Gong, Y. Xu, and Z. Liu, "Quaternion ESPRIT for direction finding with a polarization sentive array," in *Proc. International Conference on Signal Processing*, 2008, pp. 378–381.

[25] X. Zhang, C. Chen, J. Li, and D. Xu, "Blind DOA and polarization estimation for polarization-sensitive array using dimension reduction MUSIC," *Multidimensional Systems and Signal Processing*, vol. 25, no. 1, pp. 67–82, 2014.

[26] H. Chen, C. Hou, W. Liu, W.-P. Zhu, and M. Swamy, "Efficient two-dimensional direction-of-arrival estimation for a mixture of circular and noncircular sources," *IEEE Sensors Journal*, vol. 16, no. 8, pp. 2527–2536, 2016.

[27] K.-C. Ho, K.-C. Tan, and W. Ser, "An investigation on number of signals whose directions-of-arrival are uniquely determinable with an electromagnetic vector sensor," *Signal Processing*, vol. 47, no. 1, pp. 41–54, 1995.

[28] B. Hochwald and A. Nehorai, "Identifiability in array processing models with vector-sensor applications," *IEEE Transactions on Signal Processing*, vol. 44, no. 1, pp. 83–95, 1996.

[29] K.-C. Tan, K.-C. Ho, and A. Nehorai, "Uniqueness study of measurements obtainable with arrays of electromagnetic vector sensors," *IEEE Transactions on Signal Processing*, vol. 44, no. 4, pp. 1036–1039, 1996.

[30] K.-C. Ho, K.-C. Tan, and B. Tan, "Linear dependence of steering vectors associated with tripole arrays," *IEEE Transactions on Antennas and Propagation*, vol. 46, no. 11, pp. 1705–1711, 1998.

[31] K. T. Wong and M. D. Zoltowski, "Closed-form direction finding and polarization estimation with arbitrarily spaced electromagnetic vector-sensors at unknown locations," *IEEE Transactions on Antennas and Propagation*, vol. 48, no. 5, pp. 671–681, 2000.

[32] K.-C. Tan, K.-C. Ho, and A. Nehorai, "Linear independence of steering vectors of an electromagnetic vector sensor," *IEEE Transactions on Signal Processing*, vol. 44, no. 12, pp. 3099–3107, 1996.

[33] Y. Hua, "A pencil-MUSIC algorithm for finding two-dimensional angles and polarizations using crossed dipoles," *IEEE Transactions on Antennas and Propagation*, vol. 41, no. 3, pp. 370–376, 1993.

[34] J. Lundback and S. Nordebo, "Analysis of a tripole array for polarization and direction of arrival estimation," in *Proc. IEEE Workshop on Sensor Array and Multichannel Signal Processing*, July 2004, pp. 284–288.

[35] M. B. Hawes, W. Liu, and L. Mihaylova, "Compressive sensing based design of sparse tripole arrays," *Sensors*, vol. 15, no. 12, pp. 31 056–31 068, 2015.

[36] X. Lan, W. Liu, and H. Y. Ngan, "Joint 4-D DOA and polarization estimation based on linear tripole arrays," in *Proc. 22nd International Conference on Digital Signal Processing (DSP)*, 2017, pp. 1–5.

[37] X. Lan, W. Liu, and H. Ngan, "Study of Four-Dimensional DOA and Polarisation Estimation with Crossed-dipole and Tripole Arrays," *arXiv:2004.08469 [eess.SP]*, April 2020.

[38] H. L. Van Trees, *Optimum array processing: Part IV of detection, estimation, and modulation theory*. John Wiley & Sons, 2004.

[39] P. Stoica and A. Nehorai, "MUSIC, maximum likelihood, and Cramer-Rao bound," *IEEE Transactions on Acoustics, Speech, and Signal Processing*, vol. 37, no. 5, pp. 720–741, 1989.

[40] P. Stoica and K. C. Sharman, "Maximum likelihood methods for direction-of-arrival estimation," *IEEE Transactions on Acoustics, Speech, and Signal Processing*, vol. 38, no. 7, pp. 1132–1143, 1990.

[41] Y. Bresler and A. Macovski, "Exact maximum likelihood parameter estimation of superimposed exponential signals in noise," *IEEE Transactions on Acoustics, Speech, and Signal Processing*, vol. 34, no. 5, pp. 1081–1089, 1986.
[42] H. Abeida and J. P. Delmas, "Direct derivation of the stochastic CRB of DOA estimation for rectilinear sources," *IEEE Signal Processing Letters*, vol. 24, no. 10, pp. 1522–1526, 2017.
[43] L. Kumar and R. M. Hegde, "Stochastic Cramér-Rao bound analysis for DOA estimation in spherical harmonics domain," *IEEE Signal Processing Letters*, vol. 22, no. 8, pp. 1030–1034, 2015.
[44] W. Lv, H. Sun, X. Zhang, and D. Xu, "Reduced-dimension noncircular-capon algorithm for DOA estimation of noncircular signals," *International Journal of Antennas and Propagation*, vol. 2015, 2015.
[45] M. Jin, G. Liao, and J. Li, "Joint DOD and DOA estimation for bistatic MIMO radar," *Signal Processing*, vol. 89, no. 2, pp. 244–251, 2009.
[46] F. Roemer and M. Haardt, "Efficient 1-D and 2-D DOA estimation for non-circular sourceswith hexagonal shaped ESPAR arrays," in *Proc. IEEE International Conference on Acoustics Speech and Signal Processing*, vol. 4, 2006, pp. IV–IV.
[47] P. Stoica, E. G. Larsson, and A. B. Gershman, "The stochastic CRB for array processing: A textbook derivation," *IEEE Signal Processing Letters*, vol. 8, no. 5, pp. 148–150, 2001.
[48] A. Nehorai and E. Paldi, "Electromagnetic vector-sensor array processing," in *Digital Signal Processing Handbook*, 1998, pp. 65–1.
[49] H. Roger and R. J. Charles, "Topics in matrix analysis," 1994.

Xiang Lan received his BSc from Huazhong University of Science and Technology, China, in 2012, and his MSc and PhD from the Department of Electronic and Electrical Engineering, University of Sheffield, UK, in 2014 and 2019, respectively. He is currently working as a research associate at the same department, University of Sheffield. His research interests cover signal processing based on vector sensor arrays (beamforming and DOA estimation with polarized signals) and sparse array processing.

Wei Liu (S'01-M'04-SM'10) received his BSc and LLB. degrees from Peking University, China, in 1996 and 1997, respectively, MPhil from the University of Hong Kong in 2001, and PhD from the School of Electronics and Computer Science, University of Southampton, UK, in 2003. He then worked as a postdoc first at Southampton and later at the Department of Electrical and Electronic Engineering, Imperial College London. Since September 2005, he has been with the Department of Electronic and Electrical Engineering, University of Sheffield, UK, first as a Lecturer and then a Senior Lecturer. He has published more than 300 journal and conference papers, five book chapters, and two research monographs titled "Wideband Beamforming: Concepts and Techniques" (John Wiley, March 2010) and "Low-Cost Smart Antennas" (by Wiley-IEEE, March 2019), respectively. His research interests cover a wide range of topics in signal processing, with a focus on sensor array signal processing and its various applications, such as robotics and autonomous systems, human computer interface, radar, sonar, satellite navigation, and wireless communications.

He is a member of the Digital Signal Processing Technical Committee of the IEEE Circuits and Systems Society and the Sensor Array and Multichannel Signal Processing Technical Committee of the IEEE Signal Processing Society (Vice-Chair from Jan 2019). He was an Associate Editor for IEEE Trans. on Signal Processing (March 2015-March 2019) and is currently an Associate Editor for IEEE Access, and an editorial board member of the journal Frontiers of Information Technology and Electronic Engineering.

Henry Y.T. Ngan (S'02-M'08-SM'13) received his M.Phil. and Ph.D. degrees in electrical and electronic engineering at The University of Hong Kong (HKU), China. He was previously a Research Assistant Professor in mathematics, Hong Kong Baptist University. He has been a conference chair of IS&T Electronic Imaging 2016-2020. He is a senior member of IEEE.